Oo-site: A dashboard to visualize gene expression during *Drosophila* oogenesis reveals meiotic entry is regulated post-transcriptionally

Elliot T. Martin[1*], Kahini Sarkar[1, 4], Alicia McCarthy[1], and Prashanth Rangan[1,4*]

[1]Department of Biological Sciences/RNA Institute, University at Albany SUNY, Albany, NY 12202

[4]Black Family Stem Cell Institute, Department of Cell, Developmental, and Regenerative Biology, Icahn School of Medicine at Mount Sinai, 1 Gustave L. Levy Place, New York, NY 10029, USA

[*]Co-corresponding authors

Email: etmartin@albany.edu and prashanth.rangan@mssm.edu

Summary

Determining how stem cell differentiation is controlled has important implications for understanding the etiology of degenerative disease and designing regenerative therapies. *In vivo* analyses of stem cell model systems have revealed regulatory paradigms for stem cell self-renewal and differentiation. The germarium of the female *Drosophila* gonad, which houses both germline and somatic stem cells, is one such model system. Bulk mRNA sequencing (RNA-seq), single-cell (sc) RNA-seq, and bulk translation efficiency of mRNAs are available for stem cells and their differentiating progeny within the *Drosophila* germarium. However, visualizing those data is hampered by the lack of a tool to spatially map gene expression and translational data in the germarium. Here, we have developed Oo-site (https://www.ranganlab.com/Oo-site), a tool for visualizing bulk RNA-seq, scRNA-seq, and translational efficiency data during different stages of germline differentiation, that makes these data accessible to non-bioinformaticians. Using this tool, we recapitulated previously reported expression patterns of developmentally regulated genes and discovered that meiotic genes, such as those that regulate the synaptonemal complex, are regulated at the level of translation.

Introduction

The *Drosophila* ovary provides a powerful system to study stem cell differentiation *in vivo* (Bastock and St Johnston, 2008; Eliazer and Buszczak, 2011; Lehmann, 2012; Spradling et al., 2011). The *Drosophila* ovary consists of two main cell lineages, the germline, which ultimately gives rise to

1

eggs, and the soma, which surrounds the germline and plays a supportive role in egg development (Eliazer and Buszczak, 2011; Roth, 2001; Schüpbach, 1987; Xie and Spradling, 2000). Each stage of *Drosophila* female germline stem cell (GSC) differentiation is observable and identifiable, allowing GSC development to be easily studied (Bastock and St Johnston, 2008; Lehmann, 2012; Xie and Spradling, 1998). Specifically, female *Drosophila* GSCs undergo an asymmetric division, giving rise to another GSC and a cystoblast (CB) (**Figure 1A**) (Chen and McKearin, 2003b; McKearin and Ohlstein, 1995; Xie and Spradling, 1998). The GSC and CB are marked by a round structure called the spectrosome (**Figure 1A**) (De Cuevas and Spradling, 1998; Zaccai and Lipshitz, 1996). The CB then undergoes four incomplete divisions resulting in 2-, 4-, 8-, and finally 16-cell cysts (CC), which are marked by an extended structure called the fusome (**Figure 1A**) (Chen and McKearin, 2003a, 2003b; De Cuevas and Spradling, 1998). In the 16-CC, one of the cyst cells is specified as the oocyte, while the other 15 cells become nurse cells, which provide proteins and mRNAs to support the development of the oocyte (**Figure 1A**) (Bastock and St Johnston, 2008; Carpenter, 1975; Huynh and St Johnston, 2000, 2004; Navarro et al., 2001; Theurkauf et al., 1993). The 16-CC is encapsulated by somatic cells and buds off from the germarium, forming an egg chamber (**Figure 1A**) (Bastock and St Johnston, 2008; Forbes et al., 1996; Xie and Spradling, 2000). In each chamber, the oocyte grows as the nurse cells synthesize and then deposit mRNAs and proteins into the oocyte, which eventually gives rise to a mature egg (Bastock and St Johnston, 2008; Huynh and St Johnston, 2000).

Expression of differentiation factors, including those that regulate translation, results in progressive differentiation of GSCs to an oocyte (Blatt et al., 2020; Slaidina and Lehmann, 2014). In the CB, Bag-of-marbles (Bam) expression promotes differentiation and the transition from CB to 8-CC stage (Chen and McKearin, 2003a; McKearin and Ohlstein, 1995; Ohlstein and McKearin, 1997). In the 8-CC, RNA-binding Fox protein 1 (Rbfox1) promotes exit from the mitotic cell cycle into meiosis (Carreira-Rosario et al., 2016). Both the differentiation factors Bam and Rbfox1 affect the translation of mRNAs to promote differentiation (Carreira-Rosario et al., 2016; Li et al., 2009; Tastan et al., 2010). In addition, in 8-CCs, recombination is initiated across many cyst cells and then eventually is restricted to the specified oocyte (Hinnant et al., 2020; Huynh and St Johnston, 2000). Neither the mRNAs that are translationally regulated during this progressive differentiation nor how recombination is temporally regulated is fully understood (Cahoon and Hawley, 2016; Carreira-Rosario et al., 2016; Flora et al., 2018; Rubin et al., 2020; Slaidina and Lehmann, 2014; Tanneti et al., 2011; Wei et al., 2014).

66   Within the germarium, the germline is surrounded by and relies on distinct populations of somatic
67   cells for signaling, structure, and organization (Roth, 2001; Schüpbach, 1987; Xie and Spradling,
68   2000, 1998). For example, the terminal filament, cap, and anterior-escort cells act as a somatic
69   niche for the GSCs (Decotto and Spradling, 2005; Lin and Spradling, 1993; Wang and Page-
70   McCaw, 2018; Xie and Spradling, 2000). Once GSCs divide to give rise to CBs, posterior escort
71   cells guide CB differentiation by encapsulating the CB and the early-cyst stages (Kirilly et al.,
72   2011; Shi et al., 2021; Upadhyay et al., 2016). Follicle stem cells (FSCs), which are present
73   towards the posterior of the germarium, divide and differentiate to give rise to follicle cells, (FCs)
74   which surround the late-stage cysts that give rise to egg chambers (Margolis and Spradling, 1995;
75   Nystul and Spradling, 2010; Rust et al., 2020). FSCs also give rise to stalk cells and polar cells
76   which connect the individual egg chambers that comprise the ovariole (Margolis and Spradling,
77   1995; Nystul and Spradling, 2010; Rust et al., 2020; Sahai-Hernandez et al., 2012).

78

79   While there is a wealth of bulk RNA-seq, single-cell mRNA-seq (scRNA-seq), and translational
80   efficiency data from polysome-seq experiments for the cells in the germarium, there are several
81   hurdles for easy utilization of this data:

82

83   1. scRNA-seq has exquisite temporal resolution but it can miss some lowly expressed
84   transcripts which are better captured by bulk RNA-seq (Lähnemann et al., 2020).
85   However, there is no easy way to compare these two data sets.
86   2. While scRNA-seq provides mRNA levels, it does not indicate if these mRNAs are
87   translated, especially in the germline where translation control plays an important role
88   (Blatt et al., 2020; Slaidina and Lehmann, 2014).
89   3. Lastly, there is a barrier to the visualization of the data for those who are not experienced
90   in bioinformatics.

91

92   Here, we have developed a tool that we call Oo-site which integrates bulk RNA-seq, scRNA-seq,
93   and polysome-seq data to spatially visualize gene expression and translational efficiency in the
94   germarium.

95

96   **Results**
97   To make bulk RNA-, scRNA-, and polysome-, seq data accessible to the community, we have
98   collated and reprocessed previously published sequencing datasets of ovaries enriched for
99   GSCs, CBs, cysts, and egg chambers (**Figure 1B**). Notably, each genetically enriched sample

100 had matched bulk RNA-seq and polysome-seq libraries prepared, allowing for simultaneous read-
101 out of mRNA level and translation status (**Supplemental Figure 1A**). One limitation is that the
102 enriched cyst stages do not resolve each distinct stage of cyst development, instead, these
103 samples represent a mixture of cyst stages. Therefore to supplement the enrichment data, we
104 have integrated scRNA-seq data from Slaidina *et al.* which provides a more discrete temporal
105 resolution of the cyst stages (Slaidina et al., 2021). We present these data as a tool called Oo-
106 site (https://www.ranganlab.com/Oo-site), a collection of interactive visualizations that allows
107 researchers to easily input a gene or collection of genes of interest to determine their expression
108 pattern(s).

109

110 Oo-site consists of three modules: ovary-map, ovary-heatmap, and ovary-violin (**Figure 1C**). Each
111 module allows users to visualize expression from matched mRNA-seq and polysome-seq data of
112 genetically enriched stages of early GSC differentiation as well as previously published scRNA-
113 seq data (Slaidina et al., 2021). Additionally, we have integrated scRNA-seq expression data for
114 genes that cluster in somatic cell populations that reside in the germarium (Slaidina et al., 2021),
115 however, here we focus on the germline (Slaidina et al., 2021). Ovary-map allows users to
116 visualize the expression of a single gene over the course of differentiation in the framework of a
117 germarium schematic, which contextualizes staging for those less familiar with *Drosophila*
118 oogenesis. Ovary-heatmap consists of a clustered, interactive heatmap of genes determined to
119 be differentially expressed that allows users to explore expression trends over-development
120 (**Figure 1B, Supplemental Figure 1B-C'**). Finally, ovary-violin allows users to visualize the
121 expression of multiple genes over the course of differentiation (**Figure 1C**). These groups of
122 genes can be selected either by a GO-term of interest or a custom list of genes supplied by the
123 user. The user can download a spreadsheet of gene expressions corresponding to the subset of
124 selected or input genes. Finally, Oo-site incorporates a reporting tool that generates a
125 downloadable report of the visualization(s) in a standardized format to facilitate their use for
126 publication (**Figure 1C**). Researchers can use these datasets to enhance hypothesis generation
127 or to confirm expression patterns observed from other methods.

128

129 Using Oo-site, we first determined if the bulk RNA-seq data that was acquired by enriching for
130 specific stages of germline development is representative of the gene expression patterns from
131 purified cell types. We compared bulk RNA-seq data obtained by enriching for GSC and CB cell
132 types without purification from somatic cells (**Figure 1C**) to the GSC and CB data from Wilcockson
133 *et al.* where they included a fluorescent-assisted cell sorting (FACS) step to eliminate somatic

134 cells so that a pure population of these germline cells was sequenced (Wilcockson and Ashe,

135 2019). We analyzed the expression of genes that Wilcockson *et al.* identified as 2-fold or more

136 down- or upregulated with a p-value < 0.01. We found that in the enriched bulk RNA-seq data

137 these genes followed similar trends as identified by Wilcockson *et al.*, indicating that despite the

138 lack of FACS purification, enrichment of cell types reproduces meaningful mRNA expression

139 changes over these stages (**Supplemental Figure 2A-A'**).

140

141 To determine if the bulk RNA-seq data recapitulates genuine changes in gene expression, we

142 compared the expression of *ribosomal small subunit protein 19b* (*RpS19b*) in bulk RNA-seq to

143 scRNA-seq data. Our bulk RNA-seq data, as well as the available scRNA-seq data indicated that

144 *RpS19b* was highly expressed in GSCs, decreased during differentiation in the cyst stages and

145 was greatly decreased in expression in early egg chambers, consistent with previous reports (**Fig**

146 **2A-B**) (McCarthy et al., 2021; Sarkar et al., 2021). To further validate this expression pattern, we

147 probed the expression of *RpS19b in vivo* using *in situ* hybridization as well as an RpS19b::GFP

148 line that is under endogenous control elements (McCarthy et al., 2021). We found that *RpS19b*

149 was present in the GSCs and diminishes in the cyst stages both at the mRNA and protein level

150 (**Figure 2C-E'**). Additionally, RpS19b::GFP expression resembled its mRNA expression

151 indicating that its dynamic expression is achieved primarily through modulating the mRNA level

152 of *RpS19b*, consistent with its moderate to high translational efficiency in early stages (**Figure**

153 **2C-D, Supplemental Figure 2B**). Thus, enriching for specific germline stages captures changes

154 to gene expression in the germline. However, we note that care should be taken in interpreting

155 bulk RNA-seq results as the data may be influenced by the somatic cells present in the samples.

156 However, simultaneous comparison with scRNA-seq can alleviate this problem.

157

158 To determine the groups of genes that change as the GSCs differentiate into an egg, we used

159 gene ontology (GO)-term analysis to probe for pathways that change at the level of RNA using

160 bulk RNA-seq data. We did not identify any significant GO-terms in genes that are differentially

161 expressed between GSCs and CBs. We found that genes with lower expression in GSCs

162 compared to differentiating cysts are enriched in the GO-term polytene chromosome puffing which

163 is consistent with GO-terms identified in Wilcockson *et al.* for genes that are expressed at lower

164 levels in GSCs than in differentiating cysts than GSCs (**Figure 3A**). We also identified the polytene

165 chromosome puffing GO-term in genes downregulated in CBs compared to cysts. Additionally,

166 we observed that several GO-terms involving peptidase activity were enriched in genes

167 upregulated in GSCs and CBs compared to cysts (**Figure 3B**). This is consistent with findings

168 suggesting that peptidases can be actively regulated during differentiation and can influence stem
169 cell fate (Han et al., 2015; Perišić Nanut et al., 2021; Tiaden et al., 2012). We found that two GO-
170 terms related to glutathione transferase activity were enriched in genes downregulated in GSCs
171 and CBs compared to ovaries from young-wildtype (young-WT) flies and in CBs compared to
172 differentiating cysts, suggesting that metabolic processes may be altered during GSC
173 differentiation. Additionally, comparison of CBs and differentiating cysts to young-WT, which
174 contain early egg chambers, indicated that downregulated genes were enriched in GO-terms
175 involving vitelline and eggshell coat proteins (**Figure 3A**).

176

177 Next, to determine if our data could resolve large-scale expression changes that occur during
178 oogenesis we examined the expression of genes in the GO-term meiotic cell cycle. Meiosis is
179 initiated during the cyst stages of differentiation and therefore we would expect genes in the
180 category, in general, to increase in expression in the >*bam* RNAi; hs-*bam* samples (Carpenter,
181 1979; Tanneti et al., 2011). We were surprised to find no significant change in the mean mRNA
182 expression of genes in this GO-term in any of our enriched stages compared to enriched GSCs,
183 though this does not preclude gene expression changes for individual genes (**Supplemental
184 Figure 3A**). However, this is consistent with the observation that several factors that promote
185 meiosis I are transcribed in the GSCs and the cells that follow (McCarthy et al., 2021). This
186 suggests that, in general, a transition from a mitotic state to a meiotic state is not driven by large
187 changes in mRNA levels of meiotic genes.

188

189 As we did not see overall changes to mRNA levels of genes in the GO-term meiotic cell cycle, we
190 next examined the polysome-seq data of those genes to determine if changes in expression might
191 occur at the level of translation. Polysome-seq uses polysome profiling to separate mRNAs that
192 are associated with polysomes which form by mRNAs engagement with multiple ribosomes. To
193 quantify the degree to which an mRNA is associated with polysome fractions, we compared the
194 relative abundance of mRNAs from the polysome fractions to their relative expression using
195 corresponding input lysates to calculate a metric referred to as translational efficiency (TE).
196 Indeed, genes in the meiotic cell cycle GO-term had a significant increase in translation efficiency
197 in CBs and a more dramatic increase in cysts despite no significant changes to the overall mRNA
198 level of these genes (**Supplemental Figure 3A-B**). Based on scRNA-seq data, the expression of
199 meiotic cell cycle genes increased slightly but significantly in the 4-CC cluster with a median
200 increase in expression of 1.25 fold (**Supplemental Figure 3C**). This suggests that some genes
201 in the meiotic cell cycle GO-term may be regulated at the mRNA level, but as a group this

202   regulation is modest. This is likely because genes in this GO-term are robustly expressed even in
203   GSCs as the median mRNA level of meiotic cell cycle genes in enriched GSCs is 36.1 TPM, which
204   exceeds the 70th expression percentile among all genes in enriched GSCs.

205

206   To validate this finding, we examined *orientation disrupter* (*ord)* because it is a well-characterized
207   gene, is required for sister chromatid cohesion, and has previously been reported to peak in
208   expression as meiosis begins in *Drosophila* (Bickel et al., 1997, 1996; Khetani and Bickel, 2007).
209   Our Oo-site results suggested that *ord* mRNA was expressed before meiosis, both from bulk
210   RNA-seq (**Figure 4A**) and scRNA-seq (**Supplemental Figure 3D**) consistent with reports that
211   chromosome pairing initiates before meiotic entry (Christophorou et al., 2013; Joyce et al., 2013).
212   However, polysome-seq data were consistent with the observation that Ord protein expression
213   increases during the cyst stages due to translation (**Figure 4B**). This led us to predict that *ord*
214   mRNA would be expressed before meiosis, and that Ord protein expression would increase
215   during the cyst stages as previously observed, implying a change in the translation status of *ord*
216   mRNA. To test this, we performed fluorescent *in situ* hybridization against GFP in a fly expressing
217   Ord-GFP under the control of the *ord* promoter and 5'UTR. We visualized both the GFP protein
218   and the mRNA and observed increased expression of Ord::GFP protein but consistent *ord::GFP*
219   mRNA expression, indicating that Ord is controlled post-transcriptionally, likely at the level of
220   translation based on our polysome-seq data (**Figure 4C-D'**). This finding also underscores the
221   utility of Oo-site in exploring post-transcriptional gene expression changes.

222

223   To further determine if meiosis is regulated post-transcriptionally, we examined the expression of
224   genes in the GO-term "Double-strand break repair", which is known to occur during meiosis 1
225   (Hughes et al., 2018; Page and Hawley, 2003). Double-stranded breaks are resolved before egg
226   chamber formation (Hughes et al., 2018; Mehrotra and McKim, 2006; Page and Hawley, 2003).
227   At the level of input mRNA, we found no significant changes in the expression of genes in this
228   category compared to enriched GSCs (**Figure 5A**). From scRNA-seq data, the median expression
229   of double-strand break repair genes significantly increases, but the median increase was only
230   1.05 fold in 4-CCs and 1.06 in 8-CCs compared to the GSC/CB/2CC group (**Figure 5B**). This
231   suggests that double-strand break repair gene transcription begins in GSC stages and increases
232   modestly during the cyst stages.

233

234   In contrast, we found a significant increase in the median translational efficiency of double-strand
235   break repair genes, with a 1.20 fold increase in the median translational efficiency in enriched

CBs and a 1.56 fold increase in enriched cysts compared to enriched GSCs (**Figure 5C**). In young-WT the median fold change in translational efficiency decreased slightly but significantly compared to enriched GSCs at 0.95 fold. This is consistent with the observed progression of double-stranded break repair that occurs *in vivo*. This demonstrates that Oo-site can be used to derive insights into biological processes that may be changing during early oogenesis (Mehrotra and McKim, 2006; Page and Hawley, 2003). That key processes related to meiosis and differentiation are controlled post-transcriptionally is consistent with the importance of proteins that regulate translation such as Bam and Rbfox1 in differentiation and meiotic commitment during *Drosophila* oogenesis (Blatt et al., 2020; Carreira-Rosario et al., 2016; Flora et al., 2018; Kim-Ha et al., 1995; Li et al., 2009; Slaidina and Lehmann, 2014; Tastan et al., 2010).

Discussion

We have developed an application that facilitates analysis of bulk RNA-seq, sc RNA-seq, and polysome-seq data of early *Drosophila* oogenesis that is accessible to non-bioinformaticians. We have demonstrated its utility in representing expression at the mRNA and translation level. Additionally, we have demonstrated that it can be used to visualize the expression of groups of genes over development to facilitate hypothesis development. As with all sequencing data, care should be taken to validate findings from Oo-site as sequencing can be influenced by a myriad of factors.

We have used Oo-site to discover that key meiosis regulators such as proteins of the synaptonemal complex and proteins of the double-strand break machinery are regulated at the level of translation. This adds to our understanding of the mechanisms regulating the mitotic to meiotic transition. In future work, identifying the factors mediating the widespread post-transcriptional regulation of crucial meiotic genes and mechanistically how it drives the mitotic to meiotic transition is of high importance.

High-throughput sequencing has enabled researchers to generate more data than ever before However, the development of analysis tools that are usable without bioinformatics training that enable users to make sense of these data to generate hypotheses and novel discoveries has lagged (Shachak et al., 2007). Oo-site allows for hypothesis generation and discovery using the powerful model system of *Drosophila* oogenesis. We believe Oo-site might also have utility as a teaching and demonstration tool to introduce students to the power of genomics in developmental biology. The open-source nature of this software facilitates future tool development, which will be

crucial as more researchers delve into more data-intensive scRNA-seq, where visualization tools are limited and produce plots that may be difficult to interpret for those not versed in bioinformatics. Oo-site can be supplemented in the future to include additional data such as Cut and Run for various chromatin marks, nascent mRNA transcription using transient transcriptome sequencing or similar techniques, or protein levels from mass-spectroscopy to further extend its utility in hypothesis development.

Materials and Methods

The following RNAi stocks were used in this study; *ord-GFP* (Bickel Lab), *Rps19b::GFP* (McCarthy et al., 2021), *UAS-Dcr2;nosGAL4* (Bloomington stock #25751), *bam* RNAi (Bloomington #58178), *hs-bam*/TM3 (Bloomington #24637),

Sequencing data

Polysome-seq data were obtained from previous studies conducted by the Rangan lab. Data are available via the following GEO accession numbers:

>UAS-*tkv*   GSE171349

>*bam* RNAi   GSE171349, GSE166275

>*bam* RNAi; hs-*bam* GSE143728

Young-WT   GSE119458

Single-cell sequencing data were obtained from Slaidina et al., GEO accession: GSE162192

Code Availability

All code used in the preparation of this manuscript is available on GitHub at https://github.com/elliotmartin92/Developmental-Landscape/tree/master/Paper

303 The codebase underlying Oo-site is available on GitHub at
304 https://github.com/elliotmartin92/Developmental-Landscape/tree/master/ShinyExpresionMap
305

Antibodies

307 Mouse anti-1B1 1:20 (DSHB 1B1), rabbit anti-GFP 1:2000 (abcam, ab6556), rabbit anti-Vasa
308 1:4000 (Upadhyay et al., 2016), chicken anti-Vasa 1:4000 (Upadhyay et al., 2016)
309

Polysome-seq

311 Flies ready for heat shock were placed at 37°C for 2 hours, moved to room temperature for 4
312 hours, and placed back into 37°C for 2 additional hours. Flies were then left overnight at room
313 temperature and the same heat shocking procedure was repeated for a total of 2 days. Flies were
314 then dissected in 1x PBS. Polysome-seq was performed as previously described (McCarthy et
315 al., 2021).
316

Polysome-seq data processing

318 Reads were mapped to the *Drosophila* genome (dm6.01) using STAR version 2.6.1c. Mapped
319 reads were assigned to features also using STAR. Translation efficiency was calculated as in
320 (Flora et al., 2018) using an R script which is available in the Oo-site Github repo. Briefly, TPMs
321 (transcripts per million) values were calculated The $\log_2$ ratio of TPMs between the polysome
322 fraction and total mRNA was calculated as such to prevent zero counts from overly influencing
323 the data and to prevent divide by zero errors: $\frac{Polysome_{TPM}+1}{Input_{TPM}+1}$. This ratio represents TE, TE of each
324 replicate was averaged and standard error about the calculated average for each gene was
325 calculated.

326

Differential Expression

328 Differential expression analysis between all bulk RNA-seq samples in a pairwise manner was
329 performed using DEseq2 (Love et al., 2014). Differential expression was considered as
330 Foldchange > |4| fold, FDR < 0.05.

331 Differential expression analysis between all polysome-seq samples in a pairwise manner was
332 performed using DEseq2 (Love et al., 2014) using the model ~ type + genotype + genotype:type
333 with LRT (reduced = ~ type + genotype) to test for changes in polysome counts controlling for
334 input counts. Differential expression was considered as (Foldchange > |2| fold, pvalue < 0.05)

335 Differentially expressed genes between all germline clusters from scRNA-seq was determined

336 using the FindAllMarkers function from Seurat (Hao et al., 2021). Cutoff was logfc.threshold =

337 0.75.

338 Differentially expressed genes between all germarium soma clusters from scRNA-seq was

339 determined using the FindAllMarkers function from Seurat (Hao et al., 2021). Cutoff was

340 logfc.threshold = 0.75.

341

342 **GO term heatmaps**

343 GO-term enrichment analysis was performed using Panther (release 20210224) using the default

344 settings for an Overrepresentation Test of genes differentially expressed between Input samples.

345 Top 5 GO-terms based on fold enrichment of each category were plotted using ggplot2 (Wickham,

346 2016).

347

348 **Fluorescent *in situ* hybridization**

349 A modified *in situ* hybridization procedure for Drosophila ovaries was followed from Sarkar *et al*.

350 (2021). Probes were designed and generated by LGC Biosearch Technologies using Stellaris®

351 RNA FISH Probe Designer, with specificity to target base pairs of target mRNAs. Ovaries (3 pairs

352 per sample) were dissected in RNase free 1X PBS and fixed in 1 mL of 5% formaldehyde for 10

353 minutes. The samples were then permeabilized in 1mL of Permeabilization Solution (PBST+1%

354 Triton X-100) rotating in RT for 1 hour. Samples were then washed in wash buffer for 5 minutes

355 (10% deionized formamide and 10% 20x SSC in RNase-free water). Ovaries were covered and

356 incubated overnight with 1ul of the probe in hybridization solution (10% dextran sulfate, 1 mg/ml

357 yeast tRNA, 2 mM RNaseOUT, 0.02 mg/ml BSA, 5x SSC, 10% deionized formamide, and RNase-

358 free water) and primary antibody at 30°C. Samples were then washed 2 times in 1 mL wash buffer

359 with 1ul of corresponding secondary antibody for 30 minutes each and mounted in Vectashield

360 (VectaLabs).

361 **Quantification of Stainings**

362 Stainings were quantified using the Fiji Measure tool. Images were aligned and cropped to place

363 the stem cell niche at x=0. Individual cells were outlined within the germarium and Measure was

364   used to calculate the Mean intensity of staining within the cell as well as the X coordinate of the

365   centroid of the cell. Values were normalized to 1 by dividing Mean Intensity values by the

366   maximum of the Mean Intensity per germarium. Data were plotted using ggplot2 and a fit line was

367   added using ggplot2 geom_smooth with a "loess" function with default settings. The shaded area
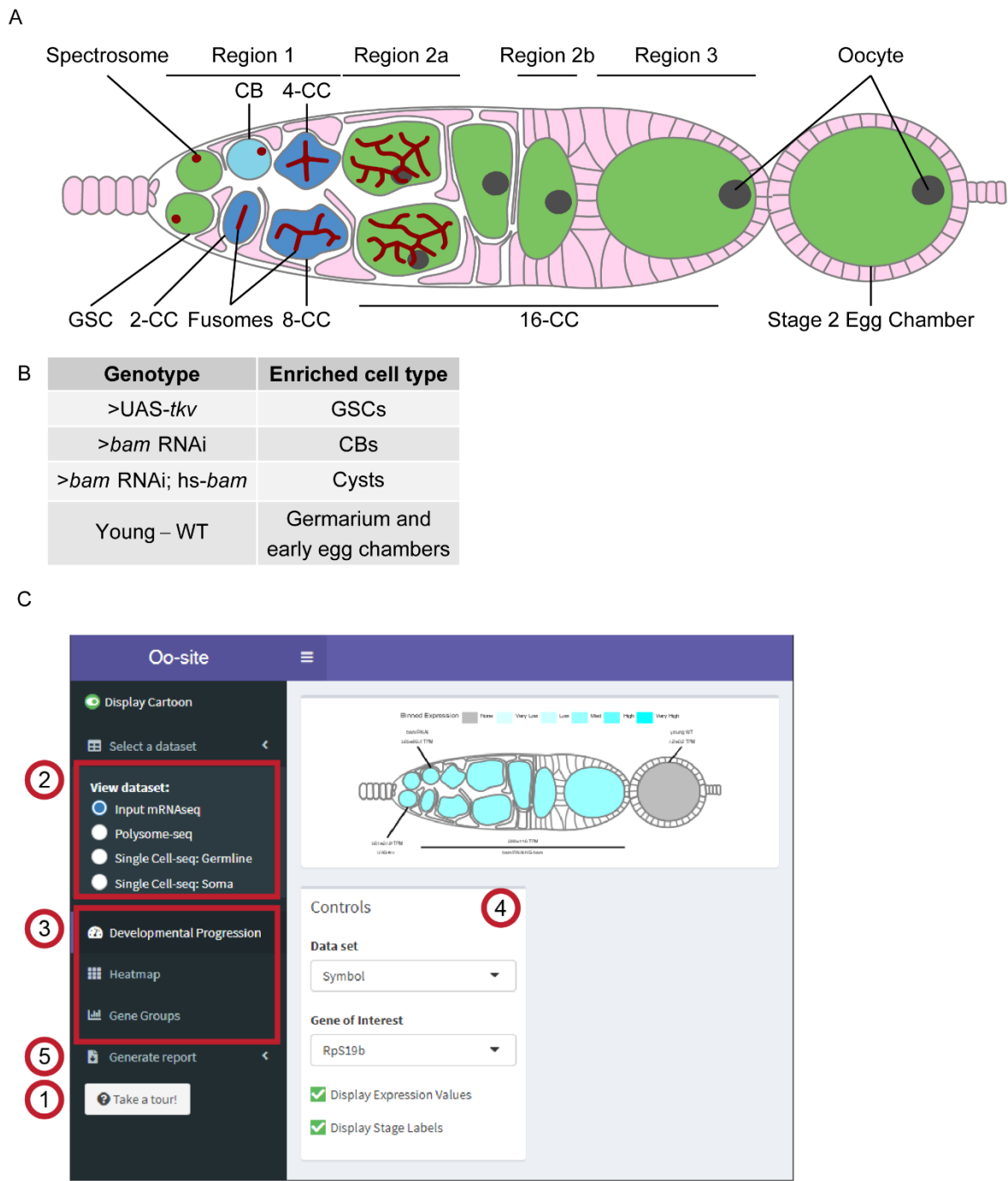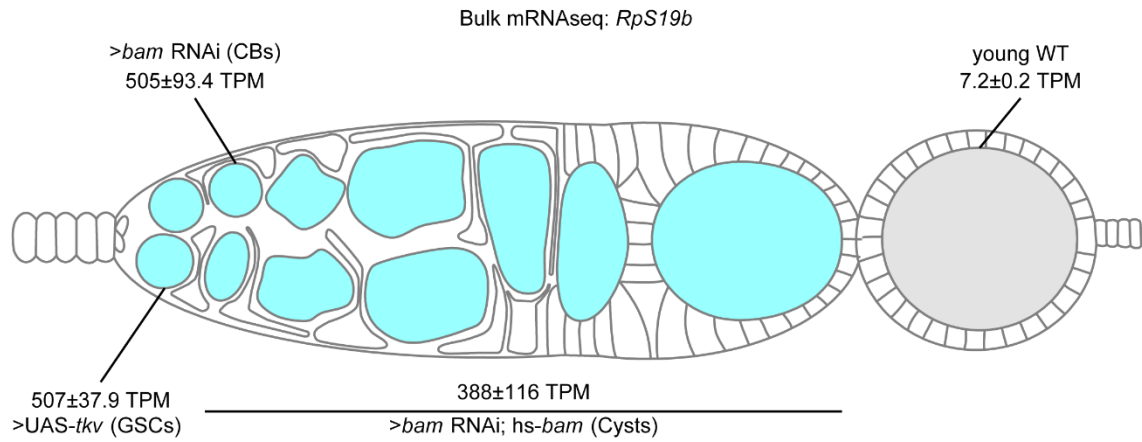
368   around the line represents standard error.

369

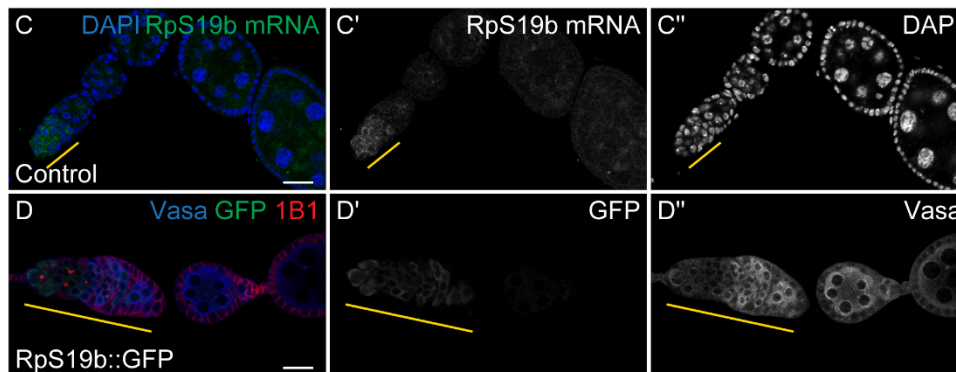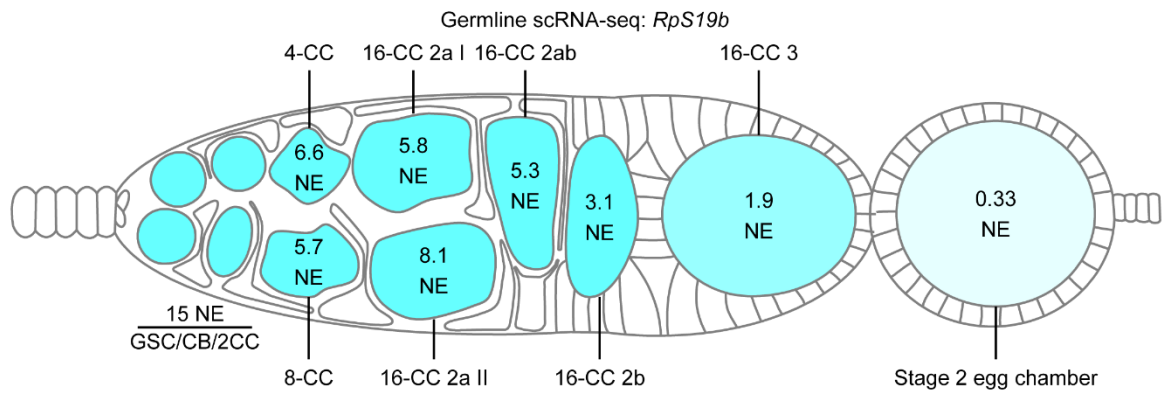370 **Figures**

A

B

Genotype	Enriched cell type
>UAS-*tkv*	GSCs
>*bam* RNAi	CBs
>*bam* RNAi; hs-*bam*	Cysts
Young – WT	Germarium and early egg chambers

C

371

372 **Figure 1: Oo-site integrates and provides an interface for interacting with multi-omic data**
373 **covering major stages of *Drosophila* GSC differentiation.**

374   (**A**) Schematic illustrating developmental stages of germline development. (**B**) Summary of the
375   samples used for bulk RNA-seq and polysome-seq and the cell types these samples are enriched
376   for. (**C**) Screenshot of Oo-site dashboard, indicating: (1) "Take a Tour!" function, which guides the
377   user through the functionality and operation of Oo-site. (2) The available seq datasets which the
378   user can view, including RNA-seq of ovaries genetically enriched for developmental stages (bulk
379   RNA-seq), polysome-seq of ovaries genetically enriched for developmental stages (Polysome-
380   seq), single-cell seq of germline stages (Single-Cell seq: Germline), and single-cell seq of somatic
381   stages in the germarium (Single-Cell seq: Soma). (3) the available visualizations which the user
382   can use, including viewing the expression of genes over development at the level of a single gene
383   (Developmental Progression), viewing all significantly changing genes as heatmaps (Heatmap),
384   and viewing groups of genes either derived from GO-term categories or supplied by the user
385   (Gene Groups). (4) The control panel, which the user can use to control the current visualization,
386   and (5) the Generate Report Function, which can be used to download a PDF report of either the
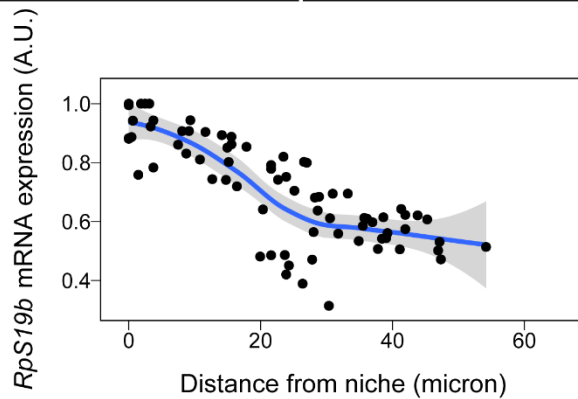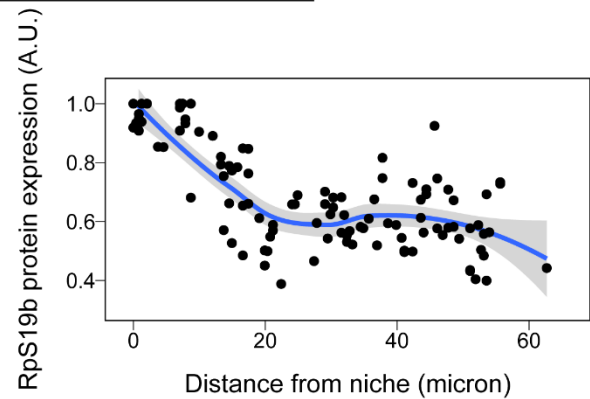387   current visualization or all active visualizations.
388

A

Bulk mRNAseq: *RpS19b*

>*bam* RNAi (CBs)
505±93.4 TPM

young WT
7.2±0.2 TPM

507±37.9 TPM
>UAS-*tkv* (GSCs)

388±116 TPM
>*bam* RNAi; hs-*bam* (Cysts)

B

Germline scRNA-seq: *RpS19b*

4-CC   16-CC 2a I   16-CC 2ab   16-CC 3

6.6 NE   5.8 NE   5.3 NE   3.1 NE   1.9 NE   0.33 NE

5.7 NE   8.1 NE

15 NE
GSC/CB/2CC

8-CC   16-CC 2a II   16-CC 2b   Stage 2 egg chamber

C DAPI RpS19b mRNA   C' RpS19b mRNA   C" DAPI
Control

D Vasa GFP 1B1   D' GFP   D" Vasa
RpS19b::GFP

E

RpS19b mRNA expression (A.U.)

Distance from niche (micron)

E'

RpS19b protein expression (A.U.)
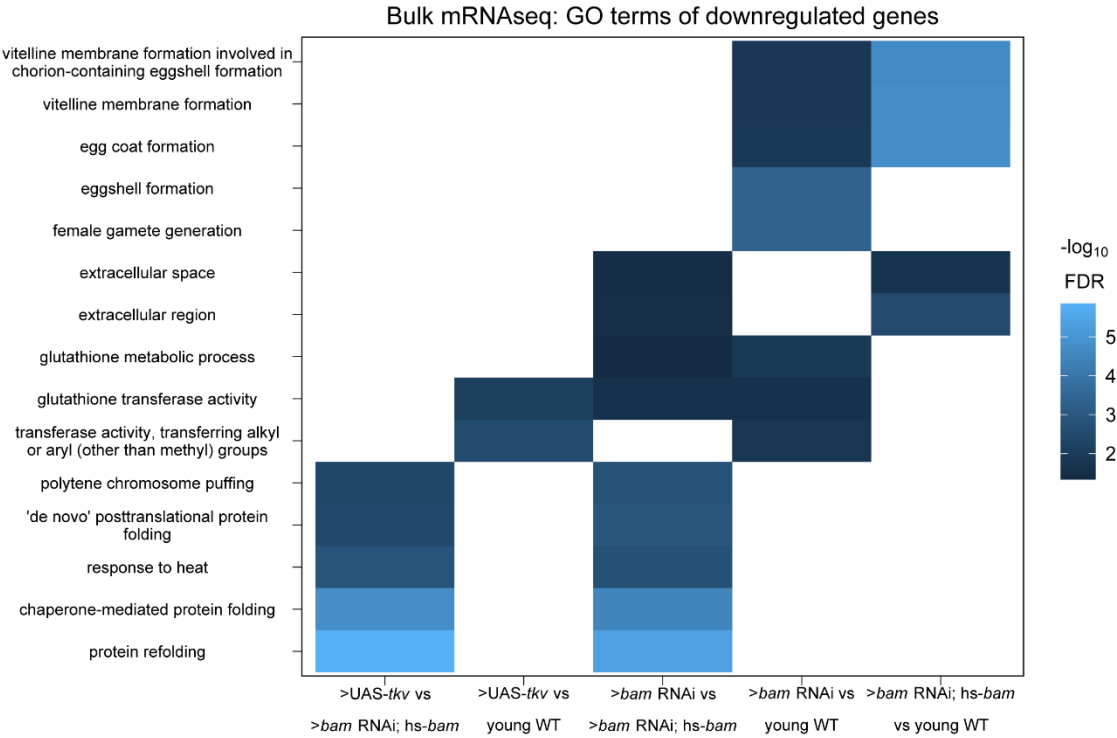
Distance from niche (micron)

389

15

Figure 2: Oo-site allows for visualization of dynamically regulated genes

(**A-B**) Visualization of expression of *RpS19b* over germline development from (A) developmentally enriched stages and (B) single-cell seq data indicate that the mRNA level of *RpS19b* decreases starting in the cysts and is dramatically decreased in early egg chambers. Color indicates relative expression and values indicate the (A) mean TPM±standard error or (B) the normalized expression of *RpS19b* in each given stage. (**C-C''**) Confocal images of ovaries with *in situ* hybridization of *RpS19b* (green, middle greyscale) and stained for DAPI (blue, right greyscale) demonstrate that the mRNA level of *RpS19b* decreases starting in the cyst stages and are dramatically lower in early egg chambers consistent with the seq data. (**D-D''**) Confocal images of ovaries expressing RpS19b::GFP, visualizing (D') GFP (green, middle greyscale), (D'') Vasa staining (blue, right greyscale), and 1B1 (red) demonstrate that the protein expression of RpS19b::GFP is consistent with its mRNA levels. (**E-E'**) Quantifications of normalized mean intensity of staining, X-axis represents the distance in microns from the niche, Y-axis represents mean intensity normalized to the maximum mean intensity per germarium of (E) *RpS19b* mRNA or (E') RpS19b::GFP. The line represents fit using a loess regression, shaded area represents the standard error of the fit. (n=5 germaria).

A

Bulk mRNAseq: GO terms of downregulated genes

B

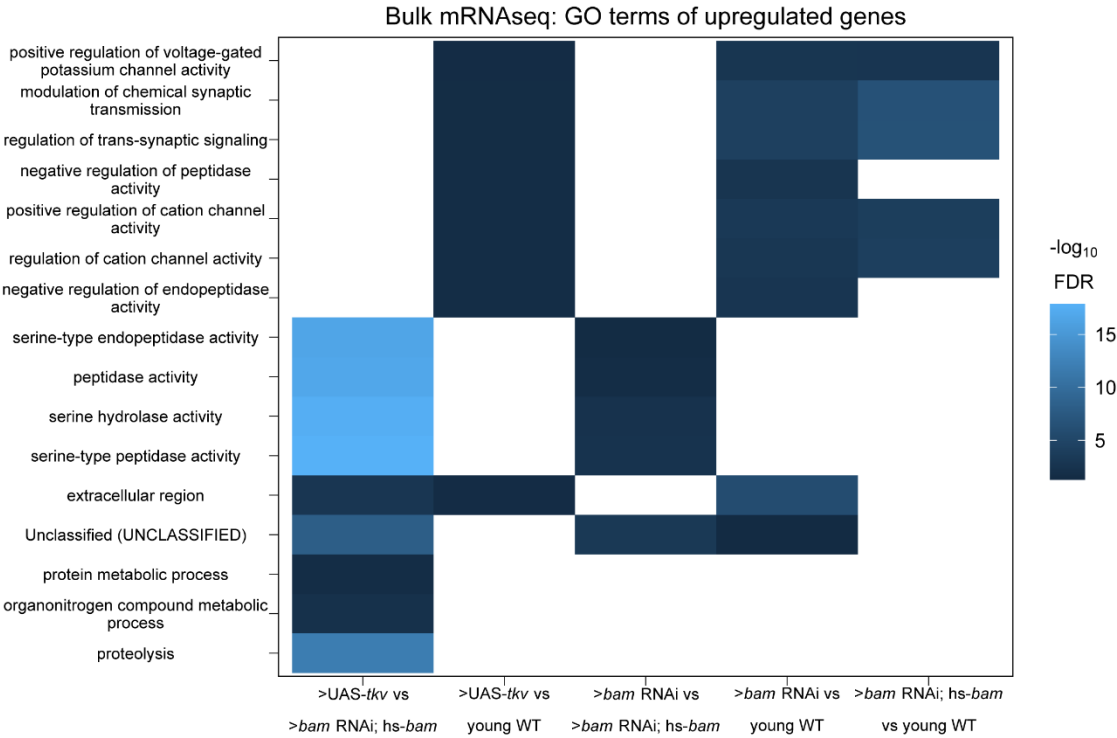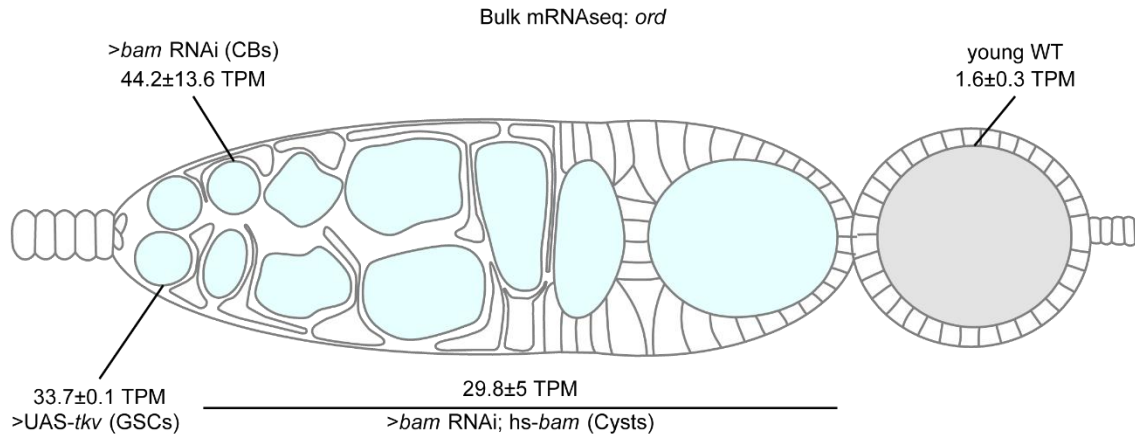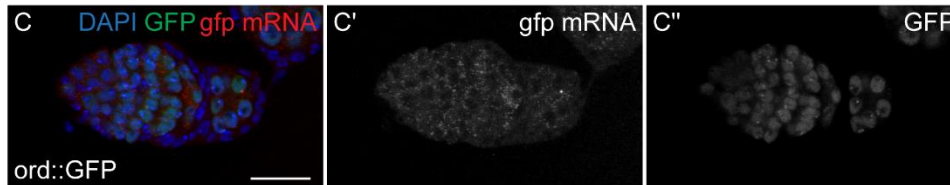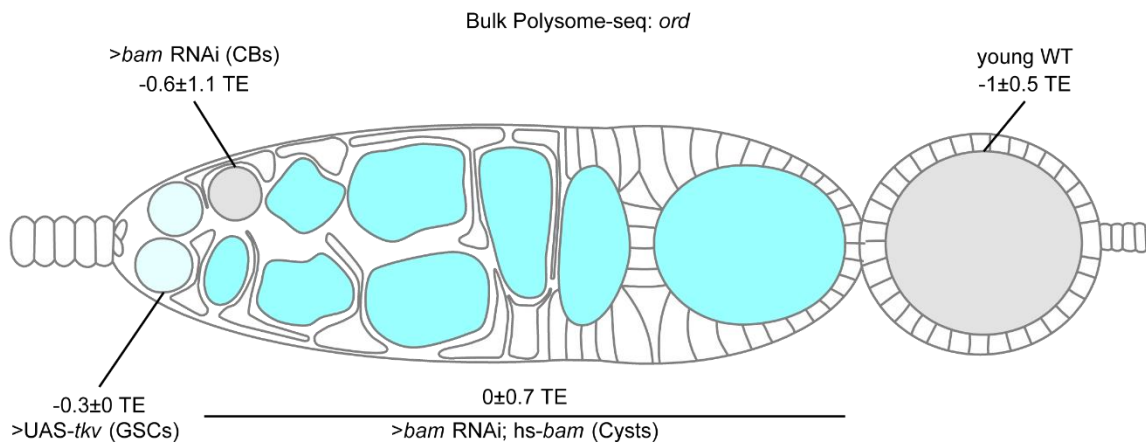## Bulk mRNAseq: GO terms of upregulated genes

406

407 **Figure 3: GO-terms enriched from differentially expressed genes between genetically**

408 **enriched developmental milestones**

409 (**A-B**) Heatmaps of top five significant GO-terms by fold enrichment resulting from each pairwise

410 comparison of significantly (A) downregulated or (B) upregulated genes in the first genotype listed

411 relative to the second genotype listed in the x-axis from bulk RNA-seq of each developmentally

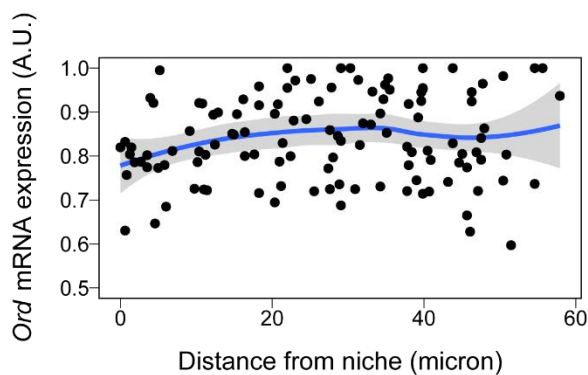412 enriched stage. Comparisons that did not generate any significant GO-terms are omitted.

413

A

Bulk mRNAseq: *ord*

>*bam* RNAi (CBs)
44.2±13.6 TPM

young WT
1.6±0.3 TPM

33.7±0.1 TPM
>UAS-*tkv* (GSCs)

29.8±5 TPM

>*bam* RNAi; hs-*bam* (Cysts)

B

Bulk Polysome-seq: *ord*

>*bam* RNAi (CBs)
-0.6±1.1 TE

young WT
-1±0.5 TE

-0.3±0 TE
>UAS-*tkv* (GSCs)

0±0.7 TE

>*bam* RNAi; hs-*bam* (Cysts)

C   DAPI GFP gfp mRNA   C'   gfp mRNA   C''   GFP
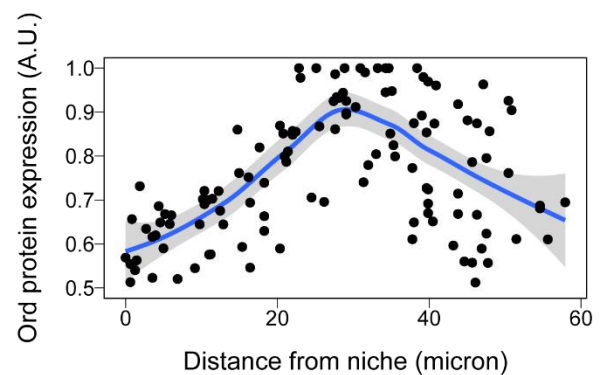
ord::GFP

D

D'

Figure 4: Ord expression is controlled post-transcriptionally

(**A-B**) Visualization of expression of *ord* over germline development from (A) bulk RNA-seq of developmentally enriched stages and (B) polysome-seq of developmentally enriched stages

418   indicates that the mRNA level of *ord* is consistent from GSCs to cysts, until decreasing in early

419   egg chambers, but the translation efficiency of *ord* increases during the cyst stages compared to

420   other stages. Color indicates (A) relative expression or (B) TE and values indicate the (A) mean

421   TPM±standard error or (B) the $\log_2$ mean TE±standard error (**C-C''**) Confocal images of ovaries

422   expressing Ord::GFP with *in situ* hybridization of *gfp* mRNA (red, middle greyscale) and stained

423   for GFP protein (green, right greyscale) and DAPI (blue) demonstrate that the mRNA level of

424   Ord::GFP is consistent throughout the germarium. (**D-D'**) Quantification of normalized mean

425   intensity of stainings (C-C''). X-axis represents the distance in microns from the niche, Y-axis

426   represents mean intensity normalized to the maximum mean intensity per germarium of *ord*

427   mRNA (D) or Ord protein (D). The line represents fit using a loess regression, shaded area

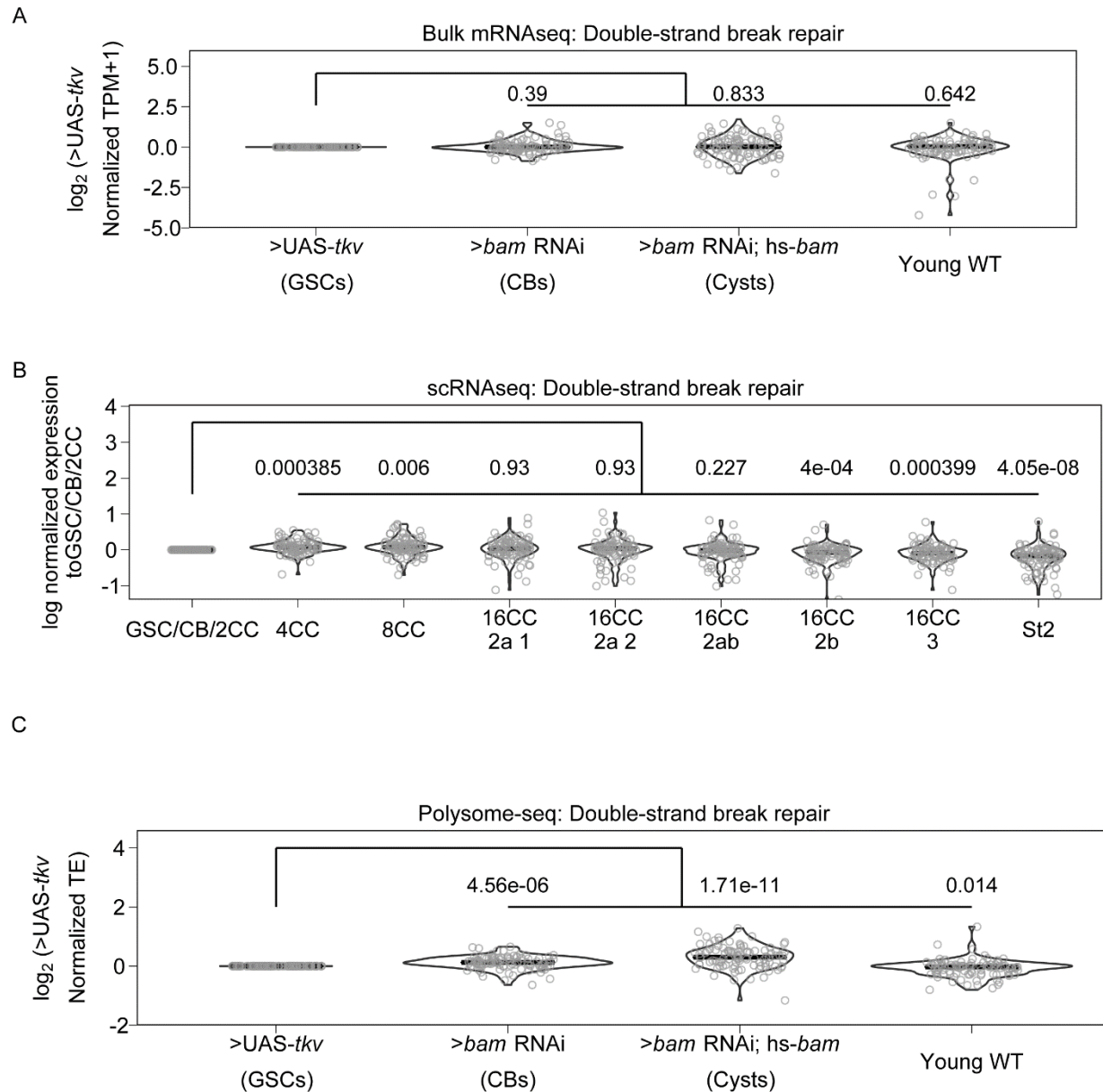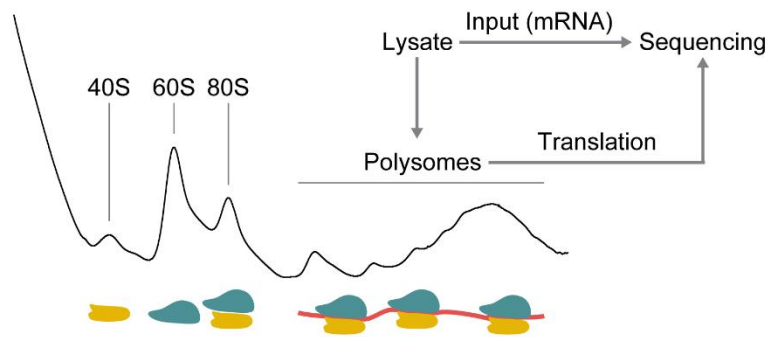428   represents the standard error of the fit. (n=8 germaria).

429

A Bulk mRNAseq: Double-strand break repair

B scRNAseq: Double-strand break repair

C Polysome-seq: Double-strand break repair

430

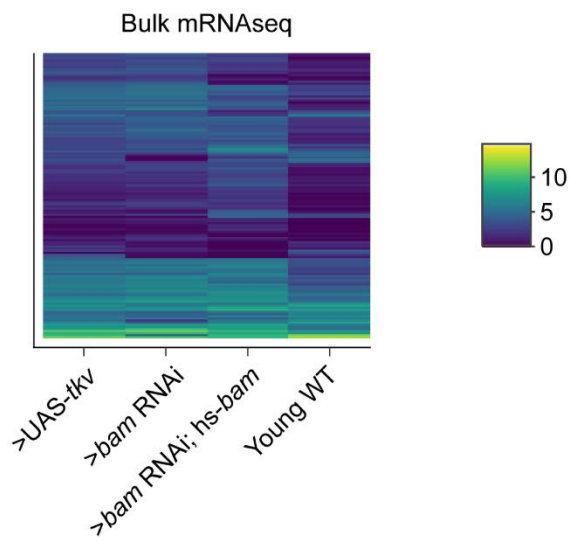**Figure 5. Genes involved in double-strand break repair may be controlled post-transcriptionally.**

(**A**) Violin plot of expression of genes in the GO category "Double-strand break repair" from bulk RNA-seq. No significant overall change in expression of these genes occurs comparing each genetically enriched developmental stage to GSCs. (**B**) Violin plot of expression of genes in the GO category "Double-strand break repair" from scRNA-seq. Overall expression of these genes increases in CBs, cysts, and young-WT ovaries compared to the GSC/CB/2CC cluster. Values above plots represent Holm-Bonnferroni adjusted p-values from a Welch's t-test between the

439   indicated genotypes (**C**) Violin plot of expression of genes in the GO category "Double-strand

440   break repair" from polysome-seq. Overall expression of these genes increases in CBs, cysts, and

441   young-WT ovaries compared to GSCs. Values above plots represent Holm-Bonnferroni adjusted

442   p-values from a Welch's t-test between the indicated genotypes.

A

40S 60S 80S

Lysate —— Input (mRNA) —→ Sequencing

Polysomes —— Translation

B **Bulk mRNAseq**

B' **Bulk Polysome-seq**

>UAS-*tkv*
>*bam* RNAi
>*bam* RNAi; hs-*bam*
Young WT

C **Germline SC-seq**

GSC/CB/2CC
4CC
8CC
16CC
16CC 2a 1
16CC 2a 2
16CC 2b
16CC 3
St2

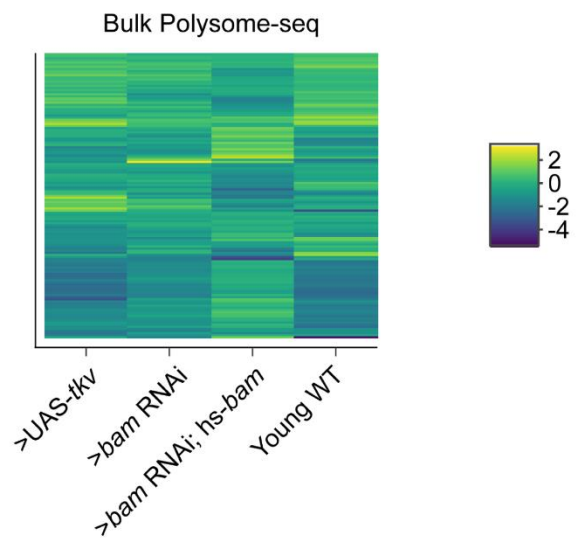C' **Soma SC-seq**

TF/CC
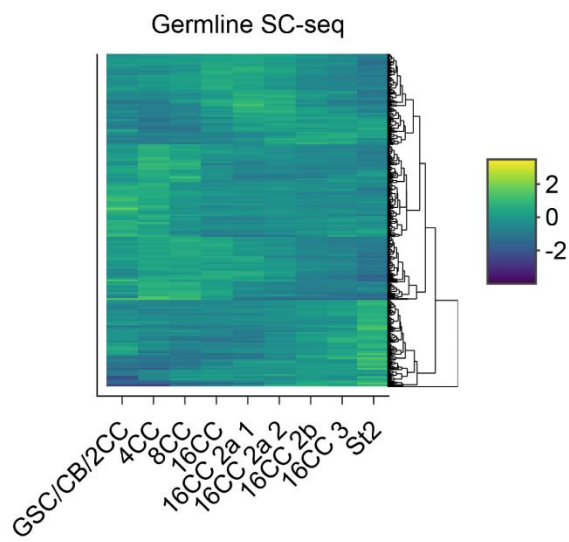aEc
cEc
pEc
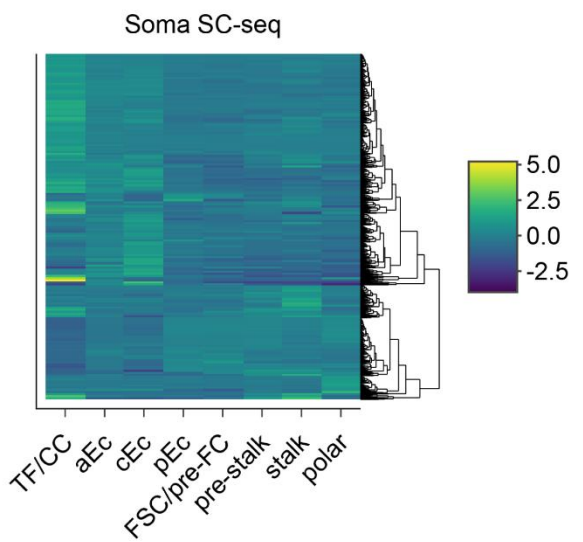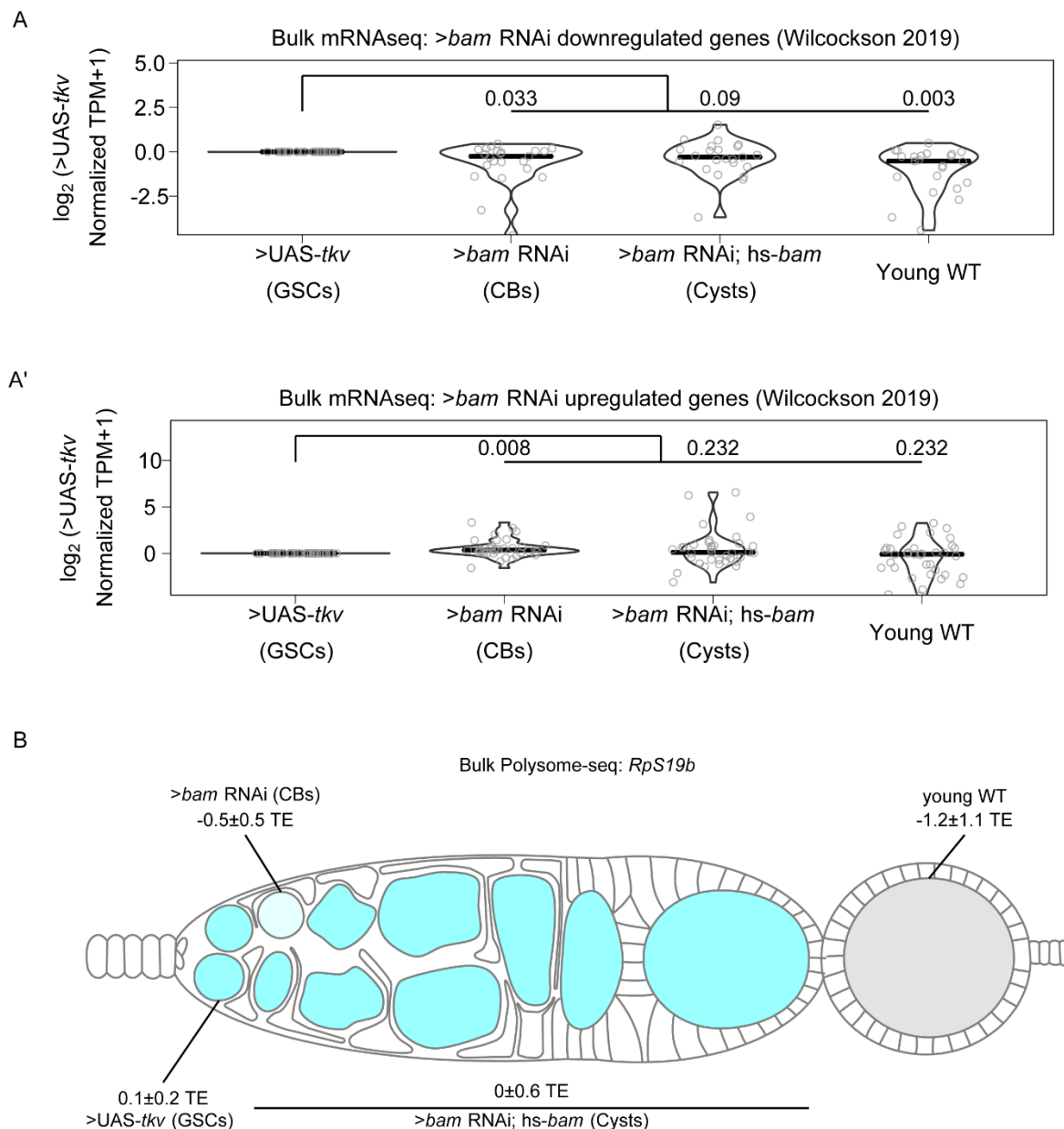FSC/pre-FC
pre-stalk
stalk
polar

443

444 **Supplemental Figure 1. Sequencing strategy and clustered heatmaps of differential**

445 **expression, related to Figure 1**
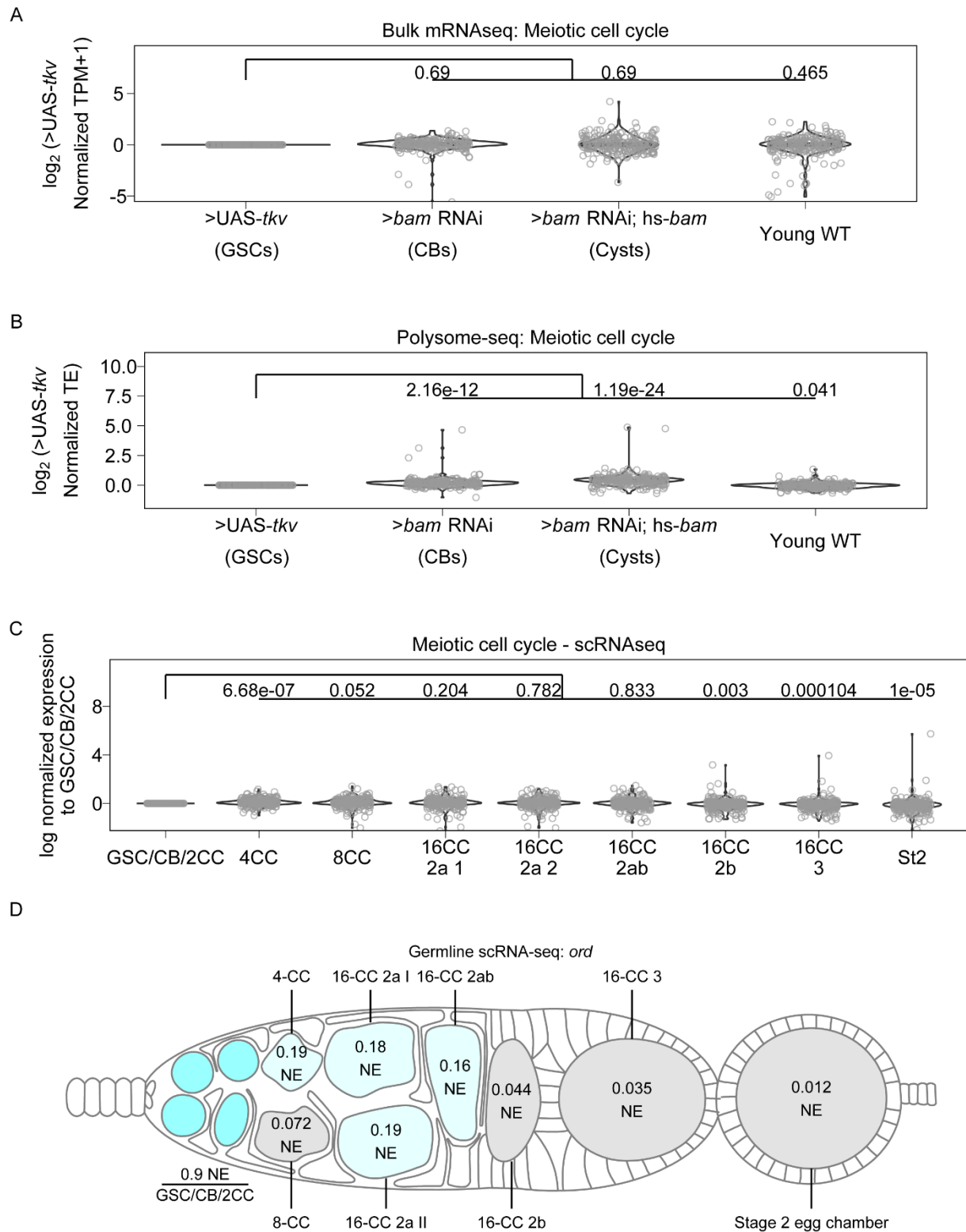
446 (**A**) Schematic of strategy used to obtain input mRNA samples and matched polysome-seq

447 libraries of ovaries genetically enriched for developmental milestones. (**B-B'**) Clustered heatmaps

448 of (B) bulk RNA-seq and (B') $\log_2$(TE) from bulk polysome-seq of the developmental milestones

449 indicated on the X-axis. Each row in the heatmap indicates a gene that is differentially expressed

450 in at least one of the milestones compared to all others in a pairwise fashion. Color scale denotes

451 average relative expression. (**C**) scRNA-seq of early germline cells and (**C'**) scRNA-seq of

452 somatic cells in the germarium. X-axis denotes cell-type and each row in the heatmap indicates

453 a gene that is differentially expressed in at least one of the cell-types compared to all others in a

454 pairwise fashion.

455

A

Bulk mRNAseq: >*bam* RNAi downregulated genes (Wilcockson 2019)

>UAS-*tkv*
(GSCs)

>*bam* RNAi
(CBs)

>*bam* RNAi; hs-*bam*
(Cysts)

Young WT

A'

Bulk mRNAseq: >*bam* RNAi upregulated genes (Wilcockson 2019)

>UAS-*tkv*
(GSCs)

>*bam* RNAi
(CBs)

>*bam* RNAi; hs-*bam*
(Cysts)

Young WT

B

Bulk Polysome-seq: *RpS19b*

>*bam* RNAi (CBs)
-0.5±0.5 TE

young WT
-1.2±1.1 TE

0.1±0.2 TE
>UAS-*tkv* (GSCs)

0±0.6 TE

>*bam* RNAi; hs-*bam* (Cysts)

456

Supplemental Figure 2. Bulk RNA-seq recapitulates previously observed expression patterns of gene expression, related to Figure 2

(**A-A'**) Violin plots of expression from bulk RNA-seq of genes 2-fold or more (A) down or (A') upregulated in bam RNAi germline cells compared to UAS-TKV overexpressing germline cell with a p-value < 0.01 over germline development from Wilcockson *et al.* demonstrate that bulk RNA-seq identifies similar trends in gene expression compared to the FACS based method employed by Wilcockson *et al.* Values above plots represent Holm-Bonnferroni adjusted p-values from a Welch's t-test between the indicated genotypes. (**B**) Visualization of expression of *RpS19b* over germline development from polysome-seq data. Color indicates TE and values indicate the $\log_2$

466   mean TE±standard error *RpS19b* TE is relatively consistent during early oogenesis and

467   decreases in the egg chambers.

468

A Bulk mRNAseq: Meiotic cell cycle

B Polysome-seq: Meiotic cell cycle

C Meiotic cell cycle - scRNAseq

D Germline scRNA-seq: *ord*

469

Supplemental Figure 3. Genes involved in meiotic cell cycle, including *ord,* may be controlled post-transcriptionally, related to Figure 4.

(**A**) Violin plots of gene expression from RNA-seq of genes in the GO-term category meiotic cell cycle. No significant overall change occurs to expression of these genes at any of the

27

developmental milestones compared to GSCs. Values above plots represent Holm-Bonnferroni adjusted p-values from a Welch's t-test between the indicated genotypes. (**B**) Violin plots of TE from polysome-seq of genes in the GO-term category meiotic cell cycle. Overall TE increases in CBs and cysts significantly compared to GSCs indicating that meiotic entry may be partially controlled post-transcriptionally. Values above plots represent Holm-Bonnferroni adjusted p-values from a Welch's t-test between the indicated genotypes. (**C**) Violin plot of expression of genes in the GO category "meiotic cell cycle" from scRNA-seq. Overall expression of these genes increases in CBs, cysts, and young-WT ovaries compared to the GSC/CB/2CC cluster. Values above plots represent Holm-Bonnferroni adjusted p-values from a Welch's t-test between the indicated genotypes. (**D**) scRNA-seq data indicate that the mRNA level of *ord* is highest in the GSC/CB/2CC cluster, but remains relatively consistent in its expression starting in the 4-CC through 16-CC 2ab clusters and is dramatically decreased in early egg chambers. Color and values indicate the normalized expression of *ord* in each given stage.

References

Bastock, R., St Johnston, D., 2008. Drosophila oogenesis. Curr. Biol. 18, R1082–R1087.

Bickel, S.E., Wyman, D.W., Miyazaki, W.Y., Moore, D.P., Orr-Weaver, T.L., 1996. Identification of ORD, a Drosophila protein essential for sister chromatid cohesion. EMBO J. 15, 1451.

Bickel, S.E., Wyman, D.W., Orr-Weaver, T.L., 1997. Mutational Analysis of the Drosophila Sister-Chromatid Cohesion Protein ORD and Its Role in the Maintenance of Centromeric Cohesion. Genetics 146, 1319–1331. https://doi.org/10.1093/genetics/146.4.1319

Blatt, P., Martin, E.T., Breznak, S.M., Rangan, P., 2020. Post-transcriptional gene regulation regulates germline stem cell to oocyte transition during Drosophila oogenesis, in: Current Topics in Developmental Biology. Elsevier, pp. 3–34.

Cahoon, C.K., Hawley, R.S., 2016. Regulating the construction and demolition of the synaptonemal complex. Nat. Struct. Mol. Biol. 23, 369–377. https://doi.org/10.1038/nsmb.3208

Carpenter, A.T.C., 1979. Synaptonemal Complex and Recombination Nodules in Wild-Type Drosophila melanogaster Females. Genetics 92, 511.

Carpenter, A.T.C., 1975. Electron microscopy of meiosis in Drosophila melanogaster females. Chromosoma 51, 157–182. https://doi.org/10.1007/BF00319833

Carreira-Rosario, A., Bhargava, V., Hillebrand, J., Kollipara, R.K.K., Ramaswami, M., Buszczak, M., 2016. Repression of Pumilio Protein Expression by Rbfox1 Promotes Germ Cell Differentiation. Dev. Cell 36, 562–571. https://doi.org/10.1016/j.devcel.2016.02.010

Chen, D., McKearin, D., 2003a. Dpp Signaling Silences bam Transcription Directly to Establish Asymmetric Divisions of Germline Stem Cells. Curr. Biol. 13, 1786–1791. https://doi.org/10.1016/J.CUB.2003.09.033

Chen, D., McKearin, D.M., 2003b. A discrete transcriptional silencer in the bam gene determines asymmetric division of the Drosophila germline stem cell. Development 130, 1159–1170. https://doi.org/10.1242/dev.00325

Christophorou, N., Rubin, T., Huynh, J.-R., 2013. Synaptonemal Complex Components Promote Centromere Pairing in Pre-meiotic Germ Cells. PLOS Genet. 9, e1004012. https://doi.org/10.1371/journal.pgen.1004012

517 De Cuevas, M., Spradling, A.C., 1998. Morphogenesis of the Drosophila fusome and its
518   implications for oocyte specification. Development 125, 2781 LP – 2789.
519 Decotto, E., Spradling, A.C., 2005. The Drosophila ovarian and testis stem cell niches: similar
520   somatic stem cells and signals. Dev. Cell 9, 501–510.
521   https://doi.org/10.1016/j.devcel.2005.08.012
522 Eliazer, S., Buszczak, M., 2011. Finding a niche: studies from the Drosophila ovary. Stem Cell
523   Res. Ther. 2, 45. https://doi.org/10.1186/scrt86
524 Flora, P., Wong-Deyrup, S.W., Martin, E.T., Palumbo, R.J., Nasrallah, M., Oligney, A., Blatt, P.,
525   Patel, D., Fuchs, G., Rangan, P., 2018. Sequential regulation of maternal mRNAs
526   through a conserved cis-acting element in their 3′ UTRs. Cell Rep. 25, 3828–3843.
527 Forbes, A.J., Lin, H., Ingham, P.W., Spradling, A.C., 1996. hedgehog is required for the
528   proliferation and specification of ovarian somatic cells prior to egg chamber formation in
529   Drosophila. Dev. Camb. Engl. 122, 1125–1135.
530 Han, R., Wang, X., Bachovchin, W., Zukowska, Z., Osborn, J.W., 2015. Inhibition of dipeptidyl
531   peptidase 8/9 impairs preadipocyte differentiation. Sci. Rep. 5, 12348.
532   https://doi.org/10.1038/srep12348
533 Hao, Y., Hao, S., Andersen-Nissen, E., Mauck, W.M., Zheng, S., Butler, A., Lee, M.J., Wilk,
534   A.J., Darby, C., Zager, M., Hoffman, P., Stoeckius, M., Papalexi, E., Mimitou, E.P., Jain,
535   J., Srivastava, A., Stuart, T., Fleming, L.M., Yeung, B., Rogers, A.J., McElrath, J.M.,
536   Blish, C.A., Gottardo, R., Smibert, P., Satija, R., 2021. Integrated analysis of multimodal
537   single-cell data. Cell 184, 3573-3587.e29. https://doi.org/10.1016/j.cell.2021.04.048
538 Hinnant, T.D., Merkle, J.A., Ables, E.T., 2020. Coordinating Proliferation, Polarity, and Cell Fate
539   in the Drosophila Female Germline. Front. Cell Dev. Biol. 0.
540   https://doi.org/10.3389/fcell.2020.00019
541 Hughes, S.E., Miller, D.E., Miller, A.L., Hawley, R.S., 2018. Female Meiosis: Synapsis,
542   Recombination, and Segregation in Drosophila melanogaster. Genetics 208, 875–908.
543   https://doi.org/10.1534/genetics.117.300081
544 Huynh, J., St Johnston, D., 2000. The role of BicD, egl, orb and the microtubules in the
545   restriction of meiosis to the Drosophila oocyte. Development 127, 2785–2794.
546   https://doi.org/10.1242/dev.127.13.2785
547 Huynh, J.-R., St Johnston, D., 2004. The Origin of Asymmetry: Early Polarisation of the
548   Drosophila Germline Cyst and Oocyte. Curr. Biol. 14, R438–R449.
549   https://doi.org/10.1016/j.cub.2004.05.040
550 Joyce, E.F., Apostolopoulos, N., Beliveau, B.J., Wu, C. -ting, 2013. Germline Progenitors
551   Escape the Widespread Phenomenon of Homolog Pairing during Drosophila
552   Development. PLOS Genet. 9, e1004013. https://doi.org/10.1371/journal.pgen.1004013
553 Khetani, R.S., Bickel, S.E., 2007. Regulation of meiotic cohesion and chromosome core
554   morphogenesis during pachytene in Drosophila oocytes. J. Cell Sci. 120, 3123–3137.
555   https://doi.org/10.1242/jcs.009977
556 Kim-Ha, J., Kerr, K., Macdonald, P.M., 1995. Translational regulation of oskar mRNA by Bruno,
557   an ovarian RNA-binding protein, is essential. Cell 81, 403–412.
558   https://doi.org/10.1016/0092-8674(95)90393-3
559 Kirilly, D., Wang, S., Xie, T., 2011. Self-maintained escort cells form a germline stem cell
560   differentiation niche. Development 138, 5087–5097. https://doi.org/10.1242/dev.067850
561 Lähnemann, D., Köster, J., Szczurek, E., McCarthy, D.J., Hicks, S.C., Robinson, M.D., Vallejos,
562   C.A., Campbell, K.R., Beerenwinkel, N., Mahfouz, A., Pinello, L., Skums, P., Stamatakis,
563   A., Attolini, C.S.-O., Aparicio, S., Baaijens, J., Balvert, M., Barbanson, B. de, Cappuccio,
564   A., Corleone, G., Dutilh, B.E., Florescu, M., Guryev, V., Holmer, R., Jahn, K., Lobo, T.J.,
565   Keizer, E.M., Khatri, I., Kielbasa, S.M., Korbel, J.O., Kozlov, A.M., Kuo, T.-H., Lelieveldt,
566   B.P.F., Mandoiu, I.I., Marioni, J.C., Marschall, T., Mölder, F., Niknejad, A., Raczkowski,
567   L., Reinders, M., Ridder, J. de, Saliba, A.-E., Somarakis, A., Stegle, O., Theis, F.J.,

568   Yang, H., Zelikovsky, A., McHardy, A.C., Raphael, B.J., Shah, S.P., Schönhuth, A.,
569   2020. Eleven grand challenges in single-cell data science. Genome Biol. 21, 31.
570   https://doi.org/10.1186/s13059-020-1926-6
571 Lehmann, R., 2012. Germline Stem Cells: Origin and Destiny. Cell Stem Cell 10, 729–739.
572   https://doi.org/10.1016/j.stem.2012.05.016
573 Li, Y., Minor, N.T., Park, J.K., McKearin, D.M., Maines, J.Z., 2009. Bam and Bgcn antagonize
574   Nanos-dependent germ-line stem cell maintenance. Proc. Natl. Acad. Sci. 106, 9304 LP
575   – 9309. https://doi.org/10.1073/pnas.0901452106
576 Lin, H., Spradling, A.C., 1993. Germline Stem Cell Division and Egg Chamber Development in
577   Transplanted Drosophila Germaria. Dev. Biol. 159, 140–152.
578   https://doi.org/10.1006/dbio.1993.1228
579 Love, M.I., Huber, W., Anders, S., 2014. Moderated estimation of fold change and dispersion for
580   RNA-seq data with DESeq2. Genome Biol. 15, 550. https://doi.org/10.1186/s13059-014-
581   0550-8
582 Margolis, J., Spradling, A., 1995. Identification and behavior of epithelial stem cells in the
583   Drosophila ovary. Development 121, 3797 LP – 3807.
584 McCarthy, A., Sarkar, K., Martin, E.T., Upadhyay, M., Jang, S., Williams, N.D., Forni, P.E.,
585   Buszczak, M., Rangan, P., 2021. MSL3 promotes germline stem cell differentiation in
586   female Drosophila. Development dev.199625. https://doi.org/10.1242/dev.199625
587 McKearin, D., Ohlstein, B., 1995. A role for the Drosophila bag-of-marbles protein in the
588   differentiation of cystoblasts from germline stem cells. Development 121, 2937 LP –
589   2947.
590 Mehrotra, S., McKim, K.S., 2006. Temporal Analysis of Meiotic DNA Double-Strand Break
591   Formation and Repair in Drosophila Females. PLOS Genet. 2, e200.
592   https://doi.org/10.1371/journal.pgen.0020200
593 Navarro, C., Lehmann, R., Morris, J., 2001. Oogenesis: Setting one sister above the rest. Curr.
594   Biol. 11, R162–R165. https://doi.org/10.1016/S0960-9822(01)00083-5
595 Nystul, T., Spradling, A., 2010. Regulation of Epithelial Stem Cell Replacement and Follicle
596   Formation in the Drosophila Ovary. Genetics 184, 503–515.
597   https://doi.org/10.1534/genetics.109.109538
598 Ohlstein, B., McKearin, D., 1997. Ectopic expression of the Drosophila Bam protein eliminates
599   oogenic germline stem cells. Development 124, 3651–3662.
600 Page, S.L., Hawley, R.S., 2003. Chromosome Choreography: The Meiotic Ballet. Science.
601   https://doi.org/10.1126/science.1086605
602 Perišić Nanut, M., Pečar Fonović, U., Jakoš, T., Kos, J., 2021. The Role of Cysteine Peptidases
603   in Hematopoietic Stem Cell Differentiation and Modulation of Immune System Function.
604   Front. Immunol. 12.
605 Roth, S., 2001. Drosophila oogenesis: Coordinating germ line and soma. Curr. Biol. 11, R779–
606   R781. https://doi.org/10.1016/S0960-9822(01)00469-9
607 Rubin, T., Macaisne, N., Huynh, J.-R., 2020. Mixing and Matching Chromosomes during Female
608   Meiosis. Cells 9, 696. https://doi.org/10.3390/cells9030696
609 Rust, K., Byrnes, L.E., Yu, K.S., Park, J.S., Sneddon, J.B., Tward, A.D., Nystul, T.G., 2020. A
610   single-cell atlas and lineage analysis of the adult Drosophila ovary. Nat. Commun. 11,
611   5628. https://doi.org/10.1038/s41467-020-19361-0
612 Sahai-Hernandez, P., Castanieto, A., Nystul, T.G., 2012. Drosophila models of epithelial stem
613   cells and their niches. WIREs Dev. Biol. 1, 447–457. https://doi.org/10.1002/wdev.36
614 Sarkar, K., Kotb, N.M., Lemus, A., Martin, E.T., McCarthy, A., Camacho, J., Iqbal, A., Valm,
615   A.M., Sammons, M.A., Rangan, P., 2021. A feedback loop between heterochromatin
616   and the nucleopore complex controls germ-cell to oocyte transition during Drosophila
617   oogenesis. https://doi.org/10.1101/2021.10.31.466575

Schüpbach, T., 1987. Germ line and soma cooperate during oogenesis to establish the dorsoventral pattern of egg shell and embryo in Drosophila melanogaster. Cell 49, 699–707. https://doi.org/10.1016/0092-8674(87)90546-0

Shachak, A., Shuval, K., Fine, S., 2007. Barriers and enablers to the acceptance of bioinformatics tools: a qualitative study. J. Med. Libr. Assoc. JMLA 95, 454. https://doi.org/10.3163/1536-5050.95.4.454

Shi, J., Jin, Z., Yu, Y., Zhang, Y., Yang, F., Huang, H., Cai, T., Xi, R., 2021. A Progressive Somatic Cell Niche Regulates Germline Cyst Differentiation in the Drosophila Ovary. Curr. Biol. 31, 840-852.e5. https://doi.org/10.1016/j.cub.2020.11.053

Slaidina, M., Gupta, S., Banisch, T.U., Lehmann, R., 2021. A single-cell atlas reveals unanticipated cell type complexity in Drosophila ovaries. Genome Res. gr.274340.120. https://doi.org/10.1101/gr.274340.120

Slaidina, M., Lehmann, R., 2014. Translational control in germline stem cell development. J. Cell Biol. 207, 13 LP – 21. https://doi.org/10.1083/jcb.201407102

Spradling, A., Fuller, M.T., Braun, R.E., Yoshida, S., 2011. Germline stem cells. Cold Spring Harb. Perspect. Biol. 3, a002642. https://doi.org/10.1101/cshperspect.a002642

Tanneti, N.S., Landy, K., Joyce, E.F., McKim, K.S., 2011. A Pathway for Synapsis Initiation during Zygotene in Drosophila Oocytes. Curr. Biol. 21, 1852–1857. https://doi.org/10.1016/j.cub.2011.10.005

Tastan, Ö.Y., Maines, J.Z., Li, Y., Mckearin, D.M., Buszczak, M., 2010. Drosophila Ataxin 2-binding protein 1 marks an intermediate step in the molecular differentiation of female germline cysts. Development 137, 3167–3176. https://doi.org/10.1242/dev.050575

Theurkauf, W.E., Alberts, B.M., Jan, Y.N., Jongens, T.A., 1993. A central role for microtubules in the differentiation of Drosophila oocytes. Dev. Camb. Engl. 118, 1169–80.

Tiaden, A.N., Breiden, M., Mirsaidi, A., Weber, F.A., Bahrenberg, G., Glanz, S., Cinelli, P., Ehrmann, M., Richards, P.J., 2012. Human serine protease HTRA1 positively regulates osteogenesis of human bone marrow-derived mesenchymal stem cells and mineralization of differentiating bone-forming cells through the modulation of extracellular matrix protein. Stem Cells Dayt. Ohio 30, 2271–2282. https://doi.org/10.1002/stem.1190

Upadhyay, M., Cortez, Y.M., Wong-Deyrup, S., Tavares, L., Schowalter, S., Flora, P., Hill, C., Nasrallah, M.A., Chittur, S., Rangan, P., 2016. Transposon Dysregulation Modulates dWnt4 Signaling to Control Germline Stem Cell Differentiation in Drosophila. PLOS Genet. 12, e1005918. https://doi.org/10.1371/journal.pgen.1005918

Wang, X., Page-McCaw, A., 2018. Wnt6 maintains anterior escort cells as an integral component of the germline stem cell niche. Dev. Camb. Engl. 145. https://doi.org/10.1242/dev.158527

Wei, Y., Reveal, B., Reich, J., Laursen, W.J., Senger, S., Akbar, T., Iida-Jones, T., Cai, W., Jarnik, M., Lilly, M.A., 2014. TORC1 regulators Iml1/GATOR1 and GATOR2 control meiotic entry and oocyte development in Drosophila. Proc. Natl. Acad. Sci. 111, E5670–E5677.

Wickham, H., 2016. ggplot2: Elegant graphics for data analysis. Springer-Verlag New York.

Wilcockson, S.G., Ashe, H.L., 2019. Drosophila Ovarian Germline Stem Cell Cytocensor Projections Dynamically Receive and Attenuate BMP Signaling. Dev. Cell 50, 296-312.e5. https://doi.org/10.1016/j.devcel.2019.05.020

Xie, T., Spradling, A.C., 2000. A Niche Maintaining Germ Line Stem Cells in the Drosophila Ovary. Science 290, 328–330. https://doi.org/10.1126/science.290.5490.328

Xie, T., Spradling, A.C., 1998. decapentaplegic Is Essential for the Maintenance and Division of Germline Stem Cells in the Drosophila Ovary. Cell 94, 251–260. https://doi.org/10.1016/S0092-8674(00)81424-5

668   Zaccai, M., Lipshitz, H.D., 1996. Differential distributions of two adducin-like protein isoforms in
669   the Drosophila ovary and early embryo. Zygote 4, 159–166.
670